Evolutionary rates of nuclear and organellar genomes are linked in land plants

Yasmin Asar[1*], Hervé Sauquet[1,2,3], and Simon Y. W. Ho[1]

[1]School of Life and Environmental Sciences, University of Sydney, Sydney, NSW 2006, Australia

[2]National Herbarium of NSW, Botanic Gardens of Sydney, Mount Annan NSW, Australia

[3]Evolution and Ecology Research Centre, School of Biological, Earth and Environmental Sciences, University of New South Wales, Sydney, NSW 2052, Australia

*Corresponding author: Yasmin Asar

Email: yasmin.asar@sydney.edu.au

ORCIDs

Yasmin Asar: https://orcid.org/0000-0002-7561-4029

Hervé Sauquet: https://orcid.org/0000-0001-8305-3236

Simon Y.W. Ho: https://orcid.org/0000-0002-0361-2307

Summary

- Plants carry genetic material in three compartments, the nuclear, mitochondrial, and chloroplast genomes. These genomes interact with each other to various degrees and are subject to shared evolutionary drivers exerted by their host organisms. However, it is not clear whether the three plant genomes display covarying evolutionary signals.
- We tested for correlated evolutionary rates between nuclear and organellar genomes using extensive data sets from the major clades of land plants (Embryophyta), including mosses, ferns, gymnosperms, and angiosperms. To examine the evolutionary dynamics in parasitic angiosperms, which are under distinctive selective pressures, we analysed data sets from mistletoes, broomrapes, sandalwoods, and rafflesias.
- Evolutionary rates of nuclear and organellar genomes were positively linked in land plants, except in the parasitic angiosperms. We also found similar positive correlations for rates of nonsynonymous and synonymous change between nuclear and organellar genomes. Our results also reveal extensive evolutionary rate variation across land plant taxa.
- Overall, we find that nuclear, mitochondrial, and chloroplast genomes in land plants share similar drivers of mutation rates, despite considerable variation in life history, morphology, and genome sizes among clades. Our findings lay the foundation for further exploration of the impact of co-evolutionary interactions on shared evolutionary rates between genomes.

Keywords: land plants, evolutionary rates, covariation, organelles, parasitic plants

Introduction

Land plants (embryophytes) colonised the terrestrial environment between 583 and 459 Myr ago (Morris *et al.*, 2018; Nie *et al.*, 2020) and have diversified into an estimated 435,000 living species (Enquist *et al.*, 2019), filling almost every ecological niche on Earth (Fig. 1). Whilst land plants display an immense range of morphological, ecological, and cellular differences, almost all have their genetic content carried in three separate genomes, found in their nuclei, mitochondria, and chloroplasts. Mitochondria are responsible for critical cell functions such as cellular respiration, immune function, and oxidative phosphorylation (Sloan *et al.*, 2014; Zervas *et al.*, 2019; Wang *et al.*, 2022). Chloroplasts are primarily responsible for photosynthesis, transforming light and water into glucose (Martin & Herrmann, 1998). Unlike the nuclear genome, chloroplasts and mitochondrial genomes are much smaller, responsible for far fewer cell functions, effectively haploid, unable to sexually recombine, and are uniparentally transmitted, usually maternally (but see Greiner *et al.,* 2015 for exceptions).

Considerable evolutionary and structural variation can be seen across the nuclear genomes of land plants, with extensive degrees of genome duplication and polyploidy. For instance, the largest known genome (1*C* = 160.45 Gb) occurs in an octoploid New Caledonian fork fern, *Tmesipteris oblanceolata* (Fernández *et al.*, 2024). Polyploidy is likely to have provided an important foundation for the phenotypic novelties that allowed the flowering plants to radiate and speciate (Soltis *et al.*, 2019; Benton *et al.*, 2022). Plant mitochondrial genomes share the same endosymbiotic origin, cellular function, and uniparental transmission as those of animals, yet they exhibit a range of structures, from circular to branched, are much larger (0.2–20 Gb), and typically have very low rates of nucleotide substitution (Wolfe *et al.*, 1987; Drouin *et al.*, 2008; Chen *et al.*, 2017; Morley & Nielsen, 2017). In contrast, chloroplast genomes are remarkably conserved in size, structure, and content across land plants. They have much lower substitution rates than nuclear genomes in land plants (Wolfe *et al.*, 1987; Drouin *et al.*, 2008; Smith, 2015). Chloroplast genomes are circular, 110–200 kb in length, and include 80–90 protein-coding genes, four ribosomal RNA genes, and 30–31 transfer RNA genes (Kaur *et al.*, 2022). However, there are massive reductions in plastome content in parasitic angiosperms (Graham *et al.*, 2017; Zervas *et al.*, 2019). This reduction reaches its most extreme in the family Rafflesiaceae, where two species have lost their entire chloroplast genome (Molina *et al.*, 2014; Cai *et al.*, 2021). Parasitic flowering plants are ‘outliers’ to the remaining land plants in other aspects; for instance, there are vastly accelerated rates of mitochondrial evolution along with gene loss in *Viscum* (mistletoes) (Havird *et al.*, 2019; Zervas *et al.*, 2019).

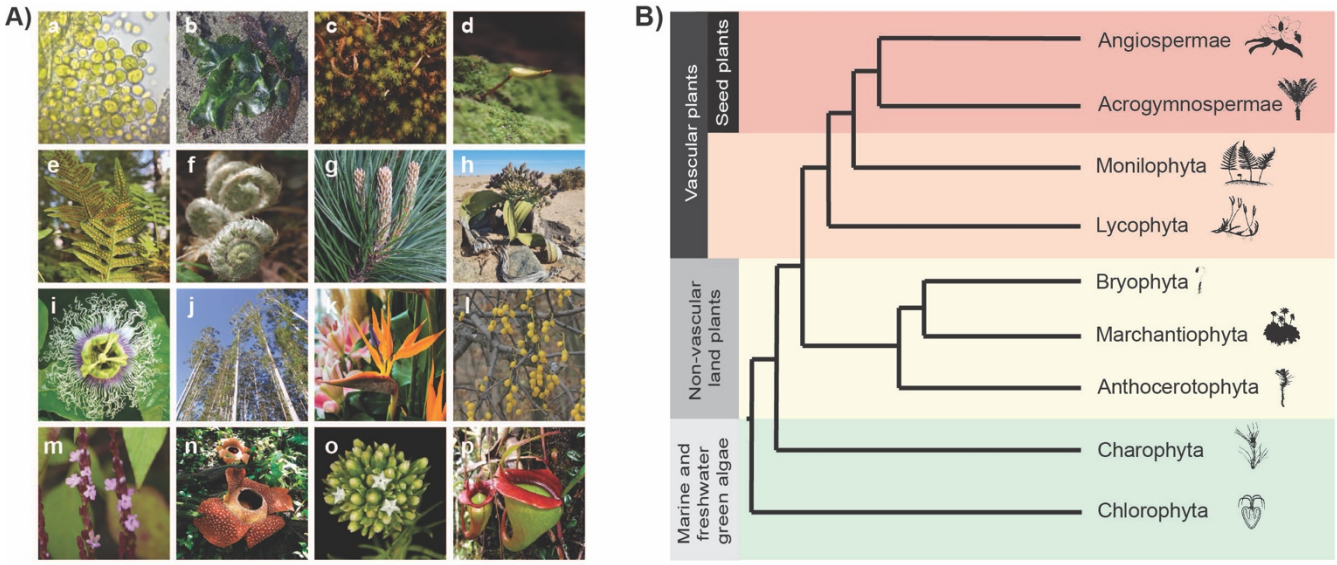

Fig. 1 Morphological diversity and phylogeny of the green plants (Viridiplantae). (A) Representatives of the major clades of land plants that were analysed in this study (c–j) and close relatives of land plants, the chlorophyte green algae (a-b). a) *Chlorella* sp., b) *Ulva* sp., c) *Takakia* sp., d) *Buxbaumia aphylla*, e) *Polypodium glycyrrhiza*, f) *Polystichium acrostichoides*, g) *Pinus radiata*, h) *Welwitschia mirabilis*, i) *Passiflora edulis*, j) *Eucalyptus grandis*, k) *Strelitzia reginae*, l) *Loranthus europaeus*, m) *Striga gesneroides*, n) *Rafflesia arnoldii*, o) *Thesium scabrum*, and p) *Nepenthes jacquelinae*. All photographs were sourced from OpenVerse (https://openverse.org). Authors and Creative Commons licenses are supplied, unless image is in the public domain: a) Owen Strickland under CC BY 4.0, b) Ryan Hodnett under CC BY-SA 4.0, f) Derek Ramsey under CC BY-SA 2.5, g) Tony Wills under CC BY 2.5, h) Marc Fradera-Soler under CC BY 4.0, i) Sam Fraser-Smith under CC BY 2.0, j) Peter Woodard under CC BY-SA 3.0, k) fotopamas under CC BY 2.0, m) Dinesh Valke under CC BY-SA 2.0, n) SofianRafflesia under CC BY-SA 4.0, o) SAplants under CC BY-SA 4.0, and p) Shawn Mayes under CC BY-SA 3.0. (B) Simplified phylogeny of Viridiplantae (the green plants). Relationships are summarised from those described in One Thousand Plant Transcriptomes Initiative (2019). Plant silhouettes are in the public domain and available at http://www.phylopic.org.

Although there are great differences in size, structure, and content between nuclear and organellar genomes, there are well-documented interactions between these genomic compartments. Coordinated change between the nucleus and mitochondria may be integral for survival; this manifests as mitonuclear covariation in animals, where the accumulation of deleterious mutations in mitochondrial genomes is compensated for by mutations in the nucleus (Martin & Herrmann, 1998; Weaver *et al.*, 2022). The mitochondria have protein complexes that consist of subunits variously encoded by the mitochondrial and nuclear proteins, and these subunits need to interact properly to ensure full function (Martin & Herrmann, 1998; Weaver *et al.*, 2022). This is particularly evident in males, where mutations that impede fertility in males are non-functional in females, and are retained in the population despite their deleterious effects (David *et al.*, 2022). Furthermore, hybrids in various animals show reduced fitness because of incompatibilities between maternally inherited mitochondrial genes and paternally inherited nuclear-encoded mitochondrial proteins (Burton *et al.*, 2013; Sloan *et al.*, 2017). Thus, mitonuclear covariation can act as a post-zygotic barrier on the path to speciation (Greiner *et al.*, 2015; Hill, 2016). This is also demonstrated in hybrid plants, where expression of chimeric open reading frames in the mitochondria causes cytoplasmic male sterility, which results in a failure to produce functional pollen (Bentolila *et al.*, 2002; Delph *et al.*, 2007; Fujii *et al.*, 2011). Only when there are compensatory changes in nuclear-encoded proteins can there be restoration of male fertility.

Given the co-evolutionary interactions between the nuclear and organellar genomes, we would expect their evolutionary rates to show some level of association. Such rate correlations have been observed in the nuclear and mitochondrial genomes of crustaceans, bivalves, mammals, yeast, and insects (Barreto *et al.*, 2018; Yan *et al.*, 2019; Piccinini *et al.*, 2021; Formaggioni *et al.*, 2022; Weaver *et al.*, 2022; Biot-Pelletier *et al.*, 2023; Tao *et al.*, 2024). However, there has been mixed evidence of evolutionary rate correlations across nuclear and organellar genomes in plants, with some researchers discounting the existence of coevolutionary interactions between nuclear and chloroplast genomes (Hill, 2020). Recent studies have found strong signals for rate correlations in data sets comprising hundreds of nuclear and chloroplast genes from 20–25 angiosperm taxa (Williams *et al.*, 2019; Forsythe *et al.*, 2021), as well as evidence for linkage disequilibrium in nuclear and mitochondrial genes across 3439 genomes of seven angiosperm species (Lian *et al.*, 2024). Similar correlations have been detected in studies of individual genera and families of angiosperms (Zhang *et al.*, 2015; Rockenbach *et al.*, 2016; Yang *et al.*, 2023; Khachaturyan *et al.*, 2024). Neverthless, the amount of co-ordination between nuclear, mitochondrial, and chloroplast genomes has not been fully explored across the diversity of land plants. This leaves uncertainty about whether

120 the interactions between the three genomes have left broad-scale signatures of covariation in their
121 evolutionary rates.
122
123 In this study, we characterise evolutionary rate variation and test for correlations in rates of nuclear,
124 mitochondrial, and chloroplast genome evolution using extensive data sets from major lineages of
125 land plants. We first conduct a simulation study to validate the performance of three phylogenetic
126 methods used to test for evolutionary rate correlations. We then use these methods to analyse data
127 sets of mosses, ferns, gymnosperms, and angiosperms. Our analyses reveal strong evolutionary rate
128 correlations between nuclear, mitochondrial, and chloroplast genes across major lineages of land
129 plants. In contrast, these patterns are not detected in parasitic angiosperms, perhaps a consequence
130 of their unique habit and reduced genomes.
131
132 **Materials and Methods**
133 *Data collection and curation*
134 We collected nucleotide sequence data for nuclear, mitochondrial, and chloroplast markers from a
135 diverse range of plant taxa, including mosses, ferns, gymnosperms, angiosperms, as well as a
136 number of genera and families of parasitic angiosperms. We use the formal terminology, as per
137 Cantino *et al.* (2007) and Bechteler *et al.* (2023). Thus, 'mosses' refers to Bryophyta, 'ferns' refers to
138 Monilophyta, 'gymnosperms' refers to the extant Acrogymnospermae, and 'angiosperms' to
139 Angiospermae. Full details of the data sets and their sources are provided in Supporting Information
140 (Table S1).
141
142 We targeted the most recent genomic studies, which included all described protein-coding genes for
143 the organellar data sets, with taxon sampling to the greatest extent achievable under our
144 computational limits. Overall, for the four major land plant clades (mosses, ferns, gymnosperms, and
145 angiosperms), we assembled data with mean alignment lengths of 167,688 bp for nuclear DNA,
146 27,341 bp for mitochondrial DNA, and 60,574 bp for chloroplast DNA. The average number of taxa
147 that were used for these comparisons was n = 86. Gene alignments were smaller for data sets of
148 parasitic angiosperms, with mean lengths of 3,298 bp, 5,585 bp, and 51,230 bp, for nuclear,
149 mitochondrial, and chloroplast data sets respectively (see Supporting Information Table S1 and
150 Notes S1). The average number of taxa for these comparisons was n = 70.
151
152 We pruned the nuclear and organellar data sets to ensure that taxa matched between the data sets.
153 We then inferred phylograms using maximum likelihood in IQ-TREE2 (version 2.2.2.6; Bui et al. 2020)

154 and Bayesian inference in BEAST2 (version 2.6.6; Bouckaert et al. 2019). For all analyses, tree
155 topologies were fixed to match those from the source studies (Supporting Information Table S1). We
156 did not allow for the possibility that separate genomic compartments can support highly divergent
157 phylogenies, but topological discordance is a source of noise that would weaken any signals of
158 evolutionary rate correlation.
159
160 *Phylogenetic analyses*
161 We inferred phylograms using maximum-likelihood analysis. When alignments of individual genes
162 were available, we selected the partitioning scheme and nucleotide substitution models in IQ-TREE2
163 (-m TESTMERGEONLY). For gene data sets with sequences that were well aligned and in frame, we
164 also split the sequences into 1st+2nd and 3rd codon sites. We used these as proxies for
165 nonsynonymous and synonymous sites, respectively, allowing us to test for correlations at these
166 sites separately. Branch lengths were proportionally linked between partitions. We constrained the
167 tree topology (-g) and inferred branch lengths for each data set.
168
169 We then inferred trees using Bayesian analysis in BEAST2, using the same partitioning schemes as in
170 the maximum-likelihood analyses. For each partition, the substitution model was averaged using
171 bModeltest (Bouckaert & Drummond, 2017). Uncorrelated lognormal relaxed clock models were
172 unlinked between genomes (nuclear, chloroplast, and mitochondrial), with one clock model having a
173 mean rate of 1.0 and with the other clock model having a mean rate that was inferred in the analysis
174 (Drummond *et al.*, 2006). The mean rate of the clock model was assigned a uniform prior with
175 bounds of 0 and 1,000,000. To allow rate variation across partitions, each was assigned its own
176 relative rate parameter. The tree topology was fixed, as in the maximum-likelihood analyses, with a
177 birth-death tree prior on the relative node times.
178
179 Each analysis was run for at least 100,000,000 MCMC steps, with sampling every 10,000 steps. The
180 sampling frequency was varied according to the chain length, with at least 10,000 trees sampled
181 from the posterior for each run. At least three independent runs were completed for each analysis
182 and their samples combined in LogCombiner, with at least 10% of each run discarded as burn-in.
183 Effective sample sizes, checked in Tracer (Rambaut *et al.*, 2018) were greater than 200 for almost all
184 parameters, including the likelihood and posterior. The combined tree samples were summarised
185 using TreeAnnotator.
186

187 *Methods for testing evolutionary rate correlations*

188 We validated the methods for detecting correlated evolutionary rates by ensuring that they were
189 both accurate (with low rate of false-positive detection) and powerful (able to detect linked rates of
190 evolution across a variety of settings). We performed a comprehensive simulation study, described
191 in the Supporting Information (see Methods S1 and Fig. S1–S6), to evaluate methods based on
192 correlations of (*i*) root-to-tip distances, (*ii*) independent sister-pair contrasts, and (*iii*) branch rates
193 inferred using Bayesian relaxed-clocks. All three methods were found to be accurate, powerful, and
194 fit for use when testing for positive evolutionary rate correlations. These results are consistent with
195 those from our previous evaluation of these methods in detecting evolutionary rate correlations
196 between molecular and morphological data sets (Asar *et al.*, 2023).

197

198 Root-to-tip distances were calculated using the package *adephylo* in R. The outgroup taxa were
199 removed from the nuclear, mitochondrial, and chloroplast phylograms inferred in our maximum-
200 likelihood analyses above, then patristic distances between the root of the tree to each tip were
201 calculated. We then tested for pairwise correlations between the root-to-tip distances of the
202 phylograms. We used a permutation correlation test (perm.cor.test function in *jmuOutlier*) (Higgins,
203 2004) using 200,000 simulations (one-sided), implemented in R (Garren, 2017), to avoid violations
204 caused by use of non-independent data points.

205

206 The second method of testing for correlated rates involved taking phylogenetically independent
207 pairs of taxa (sister-pairs) and comparing their relative branch lengths between nuclear,
208 mitochondrial, and chloroplast phylograms. Using the R package *diverge* (Anderson & Weir, 2020),
209 we extracted sister species that shared a most recent common ancestor to the exclusion of other
210 sister pairs, which avoids the problem of phylogenetic non-independence but reduces the amount of
211 data (Felsenstein, 1985; Bromham *et al.*, 2002). We computed the difference between the branch
212 lengths of sister taxa for each of the plant organellar phylograms. We tested for positive correlations
213 between these contrasts using the non-parametric Spearman's rank correlation test, to allow for
214 violations of bivariate normality and homoscedasticity. We log-transformed and standardised all
215 contrasts by dividing them by the square root of the sum of branch lengths (Garland *et al.*, 1992;
216 Freckleton, 2000; Welch & Waxman, 2008; Lanfear *et al.*, 2010). After investigating whether the data
217 met the assumptions of the independent sister-pairs contrasts method, we used a two-sample sign
218 test where the assumptions were violated. See Supporting Information for full description of
219 assumption tests and their results for all comparisons (Methods S2, Table S8–S16).

220

221 The third method of testing for correlated rates was based on the inferred posterior mean branch
222 rates from Bayesian phylogenetic analyses. We tested for positive correlations between the branch
223 rates inferred using the uncorrelated lognormal relaxed clock for the plant nuclear, mitochondrial,
224 and chloroplast data sets. We obtained the posterior mean branch rates in R, using the package
225 *treeio* (version 1.22.0) (Wang *et al.*, 2020). To compute the significance of the correlation, we used
226 Spearman's rank-order correlation test.
227
228 **Results**
229 *Evolutionary rates across land plants*
230 Our analyses revealed considerable evolutionary rate variation in nuclear and chloroplast genomes
231 across the major lineages of land plants (Fig. 2A): mosses, ferns, gymnosperms, and angiosperms.
232 We estimated evolutionary rates by dividing the mean root-to-tip distance of each phylogenetic tree
233 by the estimated age of its root node (Supporting Information Table S2). Given that the age of the
234 angiosperms continues to be debated, with molecular estimates ranging from the Late Jurassic to
235 the Permian (Sauquet *et al.*, 2022), we used multiple estimates for the crown-age of this group (Fig.
236 2A, Supporting Information Table S2). Estimated evolutionary rates of nuclear genomes ranged from
237 4.46×10^{-4} substitutions/site/Myr in acrogymnosperms to 2.16×10^{-3} substitutions/site/Myr in
238 angiosperms. In contrast, the estimated evolutionary rate of chloroplast genomes varied from
239 4.56×10^{-4} substitutions/site/Myr in acrogymnosperms to 9.67×10^{-4} substitutions/site/Myr in ferns.
240 Rates of mitochondrial genome evolution were substantially lower than those of nuclear and
241 chloroplast genomes, ranging from 2.33×10^{-4} substitutions/site/Myr in mosses to 4.69×10^{-4}
242 substitutions/site/Myr in angiosperms. All data sets of land plant nuclear, mitochondrial, and
243 chloroplast genomes used in analyses are described in Supporting Information Table S1.
244
245 Across four major lineages of land plants, we identified disparate levels of among-lineage rate
246 variation as measured by the coefficient of variation of rates (σ) (Fig. 2B). This metric was calculated
247 in a Bayesian phylogenetic analysis by dividing the standard deviation of the branch rates by the
248 mean of the branch rates, with values close to zero indicating clocklike evolution (Drummond *et al.*,
249 2006). In the major lineages of land plants, the nuclear and chloroplast data sets had similar levels of
250 moderate rate heterogeneity, with mean σ ranging from 0.694 to 1.11 across all groups (Fig. 2B;
251 Supporting Information Table S3). In angiosperms, the mitochondrial mean σ was 1.52 (95% CI 1.35–
252 1.71), reflecting an extreme degree of rate variation among lineages. Among parasitic angiosperms,
253 σ was especially pronounced in nuclear genes of Rafflesiaceae (σ = 1.60, 95% CI 0.702–2.59),

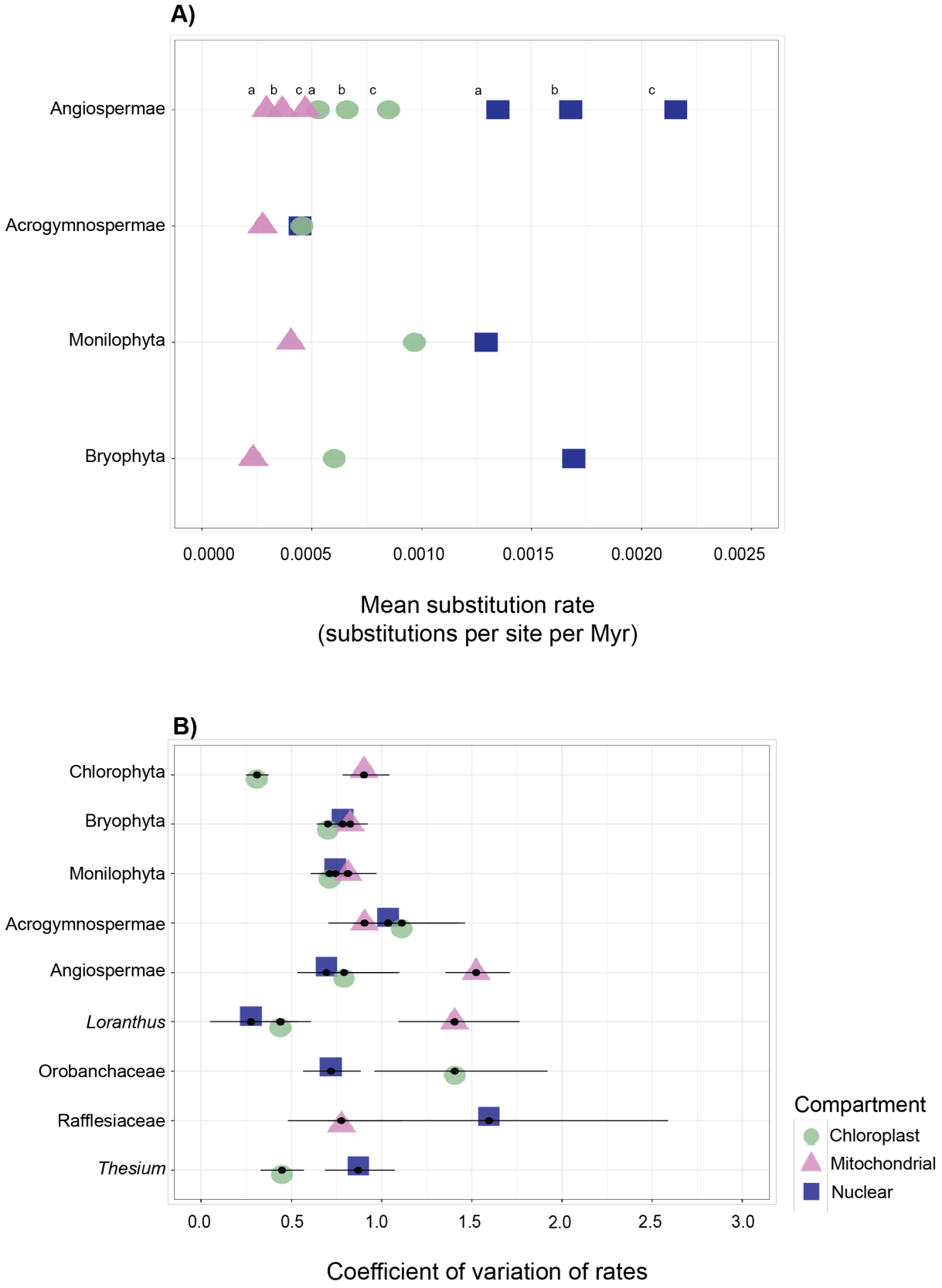
A)
Angiospermae
Acrogymnospermae
Monilophyta
Bryophyta
a b c a b c a b c
0.0000
0.0005
0.0010
0.0015
0.0020
0.0025
Mean substitution rate
(substitutions per site per Myr)
B)
Chlorophyta
Bryophyta
Monilophyta
Acrogymnospermae
Angiospermae
Loranthus
Orobanchaceae
Rafflesiaceae
Thesium
0.0
0.5
1.0
1.5
2.0
2.5
3.0
Coefficient of variation of rates
Compartment
Chloroplast
Mitochondrial
Nuclear

254

Fig. 2. There is pronounced diversity in evolutionary rates and among-lineage rate heterogeneity amongst the major lineages of land plants. (A) Estimates of evolutionary rates for nuclear markers (dark blue squares), mitochondrial markers (violet triangles), and chloroplast markers (green circles) of the major embryophyte lineages. Three estimates of evolutionary rates are provided for Angiospermae, depending on whether a Middle Triassic ~246 Ma (a), Early Jurassic ~198 Ma (b), or Late Jurassic ~ 154 Ma (c) age of origin is assumed. These age estimates are from the analyses using constrained, relaxed, and unconstrained complete calibrations reported by Ramírez-Barahona *et al.,* (2020). Plant silhouettes are in the public domain and available at http://www.phylopic.org. (B) Coefficient of variation of rates, a measure of among-lineage rate heterogeneity, estimated for each of the plant clades in this study. The nuclear, mitochondrial, and chloroplast genomic compartments are represented by dark blue squares, violet triangles, and green circles, respectively. Estimates were obtained by Bayesian relaxed-clock analysis and are shown as posterior means accompanied by 95% credibility intervals.

268 mitochondrial genes in *Loranthus* (σ = 1.40, 95% CI 1.09–1.76), and chloroplast genes in
269 Orobanchaceae (σ = 1.41, 95% CI 0.961–1.92). Concordant results were obtained when we
270 estimated the degree of among-lineage rate heterogeneity using the coefficient of variation of root-
271 to-tip distances in maximum-likelihood phylogenetic trees (Supporting Information Fig. S7, Table S3).
272
273 *Evolutionary rate correlations between genomes*
274 We tested for evolutionary rate correlations across genomic compartments of the major land plant
275 lineages using available genomic data sets (Supporting Information Table S1). We began by
276 conducting a comprehensive simulation study to validate three methods of analysis (described fully
277 in Supporting Information Methods S1): (*i*) correlations of root-to-tip distances, based on maximum-
278 likelihood phylograms; (*ii*) independent sister-pair contrasts, based on maximum-likelihood
279 phylograms; and (*iii*) correlations of branch rates inferred using Bayesian relaxed-clocks. We found
280 that all three methods were accurate, with false positives detected across an average of 3.8% of
281 replicates, and that the methods were moderately powerful, with the average detection of true
282 correlations at 88.5% (Supporting Information Fig. S1–S6). The independent sister-pair contrasts
283 method was the most conservative, being unable to detect any rate correlations when there were
284 only 18 ingroup taxa in the simulations. In these cases, there were only a small number of sister-pair
285 contrasts (n=3) (Supporting Information Fig. S1, S5). When the 18-taxon simulation setting was
286 excluded for independent sister-pair contrasts, the average detection of true correlations overall
287 increased to 99.5% across the three methods. Accordingly, we focused on sampling data sets that
288 had more than 20 ingroup taxa (Supporting Information Table S1). We found that the third method,
289 correlations of branch rates inferred using Bayesian relaxed-clocks, had the greatest accuracy and
290 power (Supporting Information Fig. S2, S6). Thus, we focus on the results obtained using this
291 method, although the two other methods yielded concordant results (Supporting Information Fig.
292 S8–S10).
293
294 We found consistently strong, significant correlations between evolutionary rates of nuclear and
295 chloroplast genomes (Fig. 3; $r_s \geq 0.48$ and $p \leq 10^{-8}$ for all comparisons). This result was found across
296 all of the major land plant lineages that we assessed. Similarly, there was a significant association
297 between evolutionary rates of nuclear and mitochondrial genomes (Supporting Information Fig. S8;
298 $r_s \geq 0.25$ and $p \leq 10^{-3}$) and between almost all mitochondrial and chloroplast genomes (Supporting
299 Information Fig. S8; $r_s \geq 0.28$ and $p < 0.01$). All tested associations were significant, with the
300 exception of angiosperm mitochondrial and chloroplast genomes, which was weakly positive but
301 statistically insignificant ($r_s = 0.032$, $p = 0.27$). We were also unable to detect an evolutionary rate

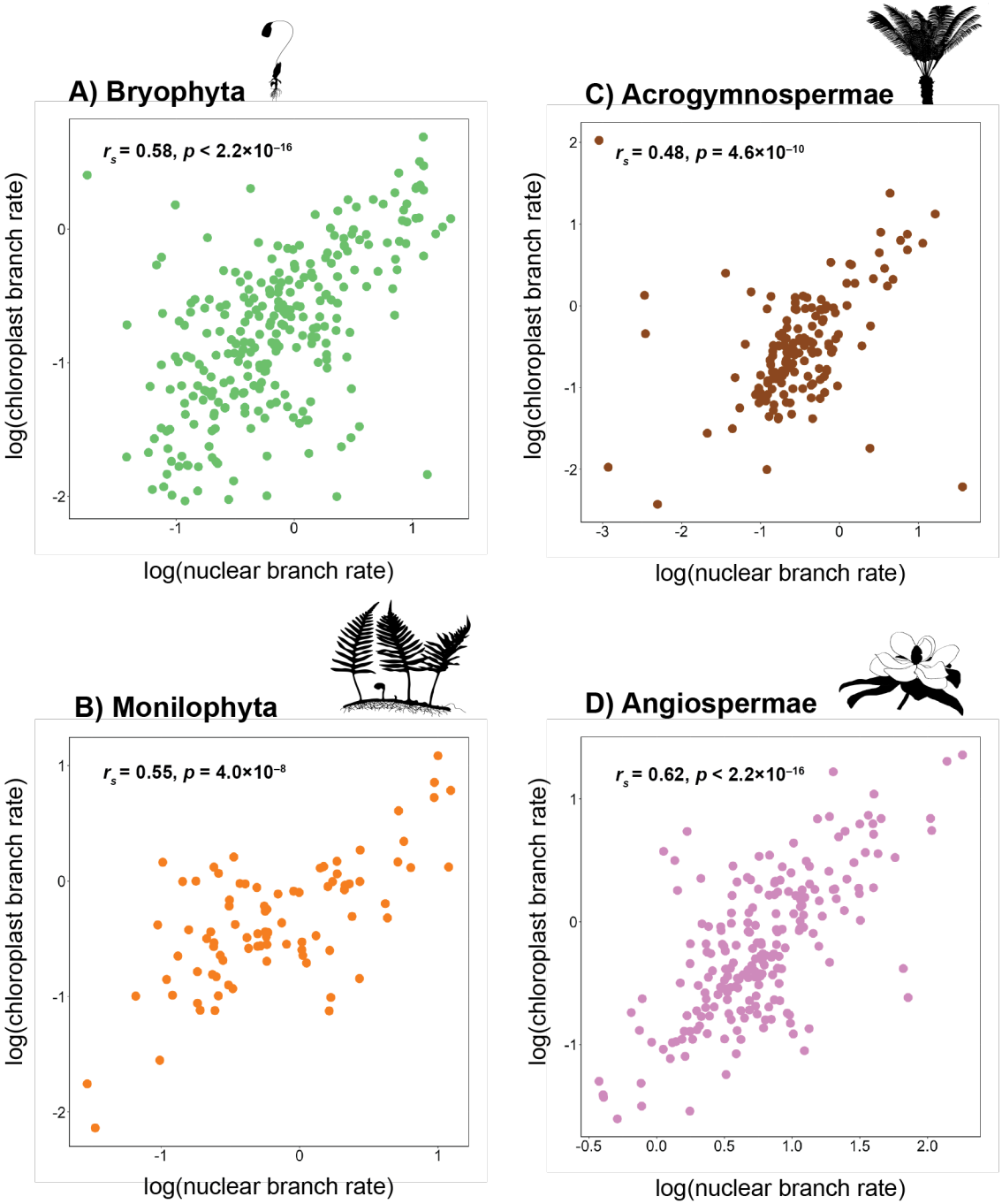

Fig. 3. Rates of nuclear and chloroplast evolution are strongly linked in the major embryophyte clades. Log-transformed relative branch rates plotted for nuclear genome against the chloroplast genome for the major land plant clades. Branch rates were estimated using Bayesian relaxed-clock analysis. The correlation coefficient (r_s) and p-value (calculated using Spearman's rank correlation test) are shown for each plot. Bold font indicates p-values below 0.05. Plant silhouettes are in the public domain and available at http://www.phylopic.org.

311 correlations between mitochondrial and chloroplast genomes in a clade of marine algae, closely
312 related to land plants, Chlorophyta (Supporting Information Fig. S11, r_s = 0.18 and p = 0.13).
313
314 To gain additional insight into the nature of the rate correlations, we performed further analyses of
315 protein-coding sequences by separating the 1st+2nd and 3rd codon sites. We treated these as
316 proxies for nonsynonymous and synonymous evolutionary changes, respectively. These analyses
317 were possible for three data sets: mosses, ferns, and angiosperms. For both nonsynonymous and
318 synonymous rates, we detected correlations between nuclear and mitochondrial genomes (Table 1;
319 $r_s \geq 0.12$ and $p \leq 0.024$) and between nuclear and chloroplast genomes (Table 1; $r_s \geq 0.51$ and $p \leq$
320 0.01). Similarly, almost all comparisons of evolutionary rates between mitochondrial and chloroplast
321 genomes detected significant associations (Table 1). However, we were unable to detect a
322 correlation in nonsynonymous rates (r_s = 0.011 and p = 0.42) and synonymous rates (r_s = 0.033 and p
323 = 0.27) between the mitochondrial and chloroplast genomes of angiosperms, despite the large
324 sample size (n = 185). The results were concordant with those obtained using the two other methods
325 that we employed (Supporting Information Table S4–S5). The ability to detect significant associations
326 was reduced when we used sister-pair contrasts, as expected from the results of our simulations.
327 However, all tested comparisons were significant when using root-to-tip distances, which was not
328 unexpected, given the slightly inflated detection of rate correlations when using this method shown
329 in our simulations (Supporting Information Methods S1, Fig. S2).
330
331 *Uncoupled evolutionary rates in parasitic flowering plants*
332 We tested for evolutionary rate correlations across the nuclear, mitochondrial, and chloroplast
333 genomes of four groups of parasitic angiosperms. For these analyses, we targeted the most recent
334 genomic or multilocus studies with large taxon sampling (full description in Supporting Information
335 Table S1 and see Notes S1). Our analyses failed to detect any associations in evolutionary rates
336 between nuclear and chloroplast genomes in Orobanchaceae, *Thesium*, and *Loranthus*, and between
337 nuclear and mitochondrial genomes in Rafflesiaceae (Fig. 4; p = 1.0). The results were largely
338 concordant with those obtained using the two other methods that we employed (Supporting
339 Information Fig. S12–S14). The only discrepancy was in *Loranthus*, for which there was a correlation
340 between the root-to-tip distances (p = 0.04); however, this comparison was based on few taxa (n =
341 13).

342 **Table 1.** Correlations between rates at 1st + 2nd sites and 3rd sites for each of the organellar
343 compartments in the major embryophyte clades. For each organellar comparison, the correlation
344 coefficient (r_s) and p-values (p) for a Spearman rank correlation test are recorded. Bold font indicates
345 p-values below 0.05.
346

Taxon[a]		**Nuclear–Chloroplast**		**Nuclear–Mitochondrial**		**Chloroplast–Mitochondrial**	
		1st + 2nd	**3rd**	**1st + 2nd**	**3rd**	**1st + 2nd**	**3rd**
Bryophyta	r_s	0.51	0.61	0.12	0.23	0.31	0.26
	p	**$<2.2\times10^{-16}$**	**$<2.2\times10^{-16}$**	**2.4×10^{-2}**	**9.4×10^{-5}**	**8.3×10^{-8}**	**7.4×10^{-6}**
Monilophyta	r_s	0.57	0.52	0.29	0.39	0.27	0.40
	p	**9.9×10^{-9}**	**2.3×10^{-7}**	**3.2×10^{-3}**	**1.2×10^{-4}**	**3.6×10^{-3}**	**2.2×10^{-5}**
Angiospermae[b]	r_s	0.40	0.30	-	-	0.011	0.033
	p	**1.1×10^{-3}**	**1.0×10^{-2}**	-	-	4.2×10^{-1}	2.7×10^{-1}

347 [a]Number of taxa (n) included for the comparisons was: n = 135 (Bryophyta), n = 44 (Monilophyta), n
348 = 51 (Monilophyta, chloroplast–mitochondrial), n = 30 (Angiospermae, nuclear–chloroplast), and n =
349 185 (Angiospermae, chloroplast–mitochondrial).
350 [b]These comparisons refer to the data sets sourced from Zeng et al., (2014), Ruhfel et al., (2014), and
351 Tyszka et al., (2023). This differs from the nuclear and chloroplast data sets presented in the main
352 figure since these did not have site partitioning data available.

353

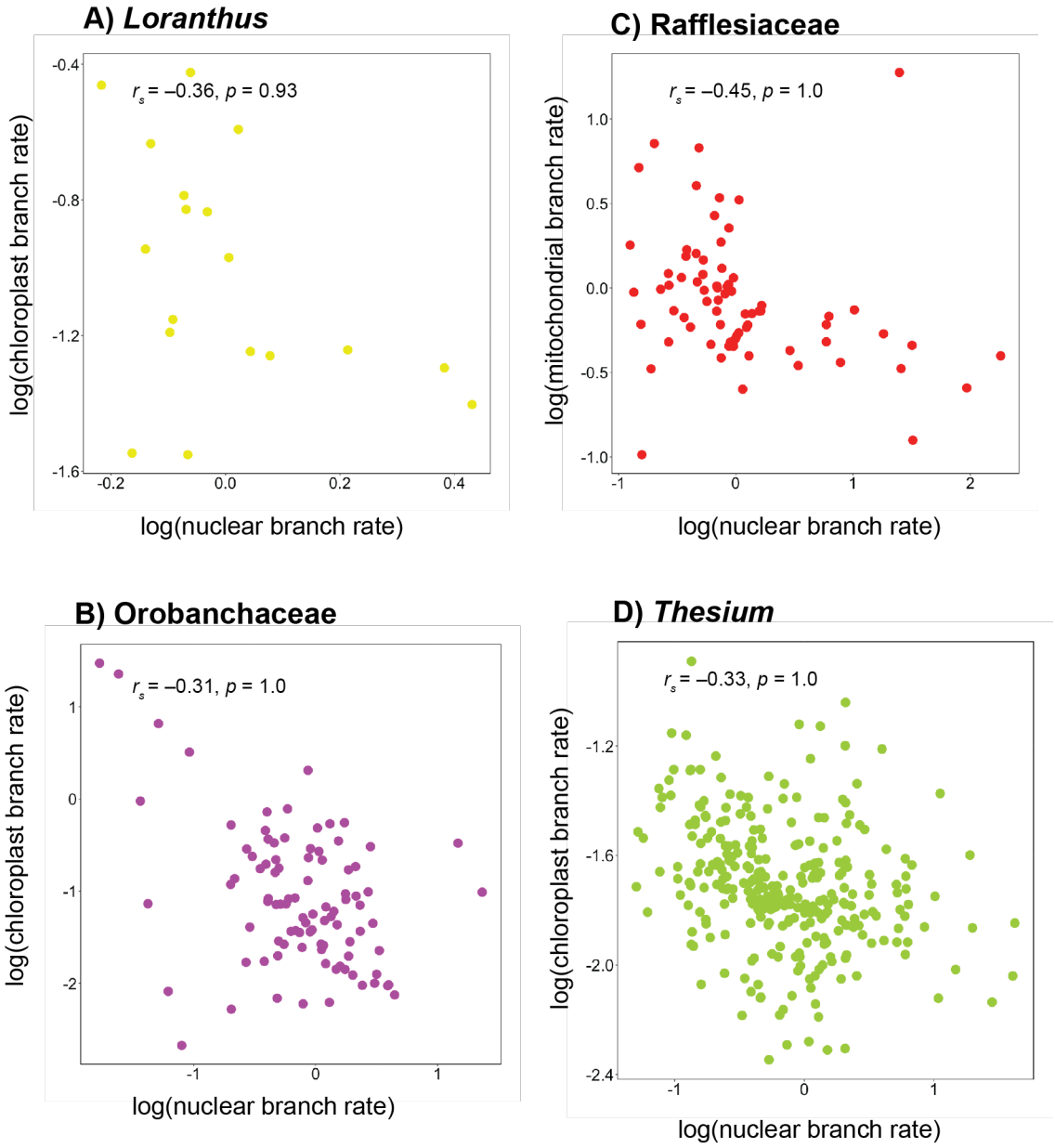

354

355 **Fig. 4.** Rates of organellar evolution are decoupled in parasitic angiosperms. Comparisons of
356 evolutionary branch rates of nuclear, mitochondrial, and chloroplast genes are shown for four
357 parasitic lineages of angiosperms. Relative branch rates were estimated using Bayesian relaxed-clock
358 analysis. The correlation coefficient (r_s) and p-value (calculated using Spearman's rank correlation
359 test) are shown for each plot. Bold font indicates p-values below 0.05.

360 **Discussion**

361 *Evolutionary rate correlations between genomes in land plants*

362 Our study has shown that evolutionary rates are positively correlated between the nuclear,
363 mitochondrial, and chloroplast genomes in the major lineages of land plants. These correlations
364 were detected using various methods of analysis that we validated through an extensive simulation
365 study. The pervasive signal of rate correlations across such diverse lineages is remarkable, given
366 their ancient age (e.g., bryophyte mosses arose 424–416 Ma; Bechteler *et al.,* 2023) and their
367 disparate life histories and ecologies. Contrastingly, we could not detect any evolutionary rate
368 correlations in parasitic angiosperms. Indeed, parasitic angiosperms feature a variety of distinctive
369 morphological and cellular traits that demarcate them from the rest of the flowering plants. For
370 instance, the 'parasite reduction syndrome' phenomenon describes the convergent loss of
371 vegetative tissue and photosynthetic organs and genes in parasitic flowering plants (Sanchez-Puerta
372 *et al.*, 2023).

373

374 Evolutionary rate correlations are consistent with the broad effects of cytonuclear covariation and
375 interaction in land plants. These results are in line with the presence of mitonuclear covariation in
376 animals (Weaver *et al.*, 2022). There is evidence that coordination between the nuclear and
377 organellar genomes in plants is vital to fundamental processes in plant cells, including ATP synthesis,
378 oxidative phosphorylation, and photosynthesis (Sloan *et al.*, 2014). For instance, in flowering plants,
379 2000 proteins are contained in the mitochondria, but fewer than 41 of these are encoded by the
380 mitochondrial genome (Chen *et al.*, 2017). The vast majority of proteins are encoded in the nucleus
381 and transferred into the mitochondria by transit peptides. The nuclear genome can thus generate
382 regulatory factors required for effective mitochondrial function (Chen *et al.*, 2017; Hill, 2020; Wang
383 *et al.*, 2022). This is particularly important in the mitochondrial response to pathogen infection,
384 activating programmed cell death, and immune function (Wang *et al.*, 2022).

385

386 Gene exchange between genomic compartments might be partly driving the evolutionary rate
387 correlation that we have uncovered. There are clear instances of bidirectional movement between
388 the nuclear and mitochondrial genomes; for example, up to half of the maize mitochondrial genome
389 is nuclear in origin (Chen *et al.*, 2017). The movement of mitochondrial genes into the chloroplast
390 genome appears to be much less profuse. The conserved chloroplast genome is more likely to
391 transfer its genes to the nuclear and mitochondrial genomes, but unable to take up foreign
392 organellar DNA (Chen *et al.*, 2017; Hill, 2020). This is consistent with the uniformity in size and
393 structure of the chloroplast genome in land plants. Furthermore, the sexually recombining nuclear

genome has taken up hundreds of genes from the organellar compartments, as well as controlling and regulating many of the functions of the mitochondria and chloroplasts (Martin, 2003; Sloan *et al.*, 2014). These features of genomic interaction suggest a weaker association between the evolutionary rates of mitochondrial and chloroplast genomes. However, if evolutionary rates in the mitochondrial and chloroplast genomes are both strongly linked to that of the nuclear genome, an indirect association can emerge between the rates of the two organellar genomes. This is consistent with the strength of the rate correlation being somewhat reduced between the two organellar compartments in ferns, angiosperms, and gymnosperms.

Our findings may also explain why higher rates of chloroplast substitution are linked to diversification in the angiosperm family Proteaceae (Duchêne & Bromham, 2013). A higher rate of change in the chloroplast genome predicts rapid changes in the nuclear and mitochondrial genomes, potentially driving adaptation, reproductive isolation, and eventually speciation. This is similar to findings in vertebrate and invertebrate animals, where mitonuclear covariation is a key factor in bolstering speciation (Hill, 2016; Wang *et al.*, 2021; Weaver *et al.*, 2022). Furthermore, a similar link between substitution rate and diversification has been found across many angiosperm clades (Lancaster, 2010; Bromham *et al.*, 2015)

Shared drivers of evolutionary rates

Although cytonuclear interactions are expected to produce some degree of evolutionary covariation between the nuclear and organellar genomes, the observed correlations in evolutionary rates might reflect a shared response by all three genomic compartments to some other factor. For example, the genomes might be responding to the same selection pressures or might have a shared system of DNA repair (Williams *et al.*, 2019). We looked for signatures of these factors by performing separate tests of correlations for nonsynonymous and synonymous sites. We found correlations between the nonsynonymous rates of nuclear and organellar genomes, consistent with positive selection and genomic interactions driving the shared variation in evolutionary rates. However, we also found correlations between the synonymous rates of nuclear and organellar genomes, suggesting that there is a shared driver of mutation rates across the three genomic compartments. This is supported by the results of a previous study that found correlated rates at synonymous sites, but not at nonsynonymous sites (Bromham *et al.*, 2015). However, our results suggest that the patterns of mutation rate variation are also being propagated to nonsynonymous rates, where a weaker correlation is apparent across the three genomes. The results of our analyses, conducted at a broad scale on hundreds of nuclear genes and tens of organellar genes, contradict those of previous

428 studies that only found correlations between mitochondrial- and nuclear-encoded mitochondrial
429 genes known to interact (Yan *et al.*, 2019; Piccinini *et al.*, 2021; Weaver *et al.*, 2022).
430
431 Previous studies have identified a number of potential drivers of mutation rates in plant genomes.
432 For instance, generation time is closely linked to long-term rates of meiosis in plants, since each
433 elapsed generation has undergone a meiotic cycle. Thus, generation time might be driving the
434 mutation rates of all three genomes (Petit & Hampe, 2006). Also, plant height is closely linked to
435 generation time, and height has been found to be strongly associated with the rate of molecular
436 evolution (Lanfear *et al.*, 2013). This may be because taller plants have slower growth in their apical
437 meristem and so undergo fewer cycles of mitosis (Li *et al.*, 1996; Lanfear *et al.*, 2013). Therefore,
438 fewer mutations are inherited by offspring, effectively reducing the evolutionary rates of taller
439 plants.
440
441 Environmental factors such as temperature can potentially act as mutagens in plants (Davies *et al.*,
442 2004; Quiroz *et al.*, 2023). This has been shown by experiments in *Arabidopsis thaliana*, where multi-
443 generational exposure to higher temperature led to accumulation of mutations in genes involved in
444 DNA repair, defense repair, and signalling, as well as increasing the mutation rate (Belfield *et al.*,
445 2021; Lu *et al.*, 2021). UV irradiation is another well-documented mutagen in plants (Davies *et al.*,
446 2004; Quiroz *et al.*, 2023), leading to oxidative DNA damage as demonstrated in Cucurbitaceae
447 (Watanabe *et al.*, 2006). These environmental drivers of mutation would potentially act on all three
448 genomes in land plants.
449
450 Population size is also likely to have a broad impact on the evolutionary dynamics of nuclear,
451 mitochondrial, and chloroplast genomes. There is less efficient selection against mutations in small
452 populations, leading to a reduction in the efficiency of DNA repair machinery and ultimately to
453 elevated mutation rates across the three genomes (Bergeron *et al.*, 2023). There is evidence of
454 unique systems of DNA repair in the nuclear, mitochondrial, and chloroplast genomes. For instance,
455 mitochondria lack nucleotide excision repair, whereas chloroplasts are unable to fix double-strand
456 breaks using non-homologous end joining (Boesch *et al.*, 2011). Genome copy number and mutation
457 rate are negatively linked in mitochondria, this may be because unmutated copies can perform
458 repairs on double-strand breaks, however, this pattern is not seen in chloroplasts (Zwonitzer *et al.*,
459 2024). Alternatively, there is mounting evidence for strong links between the epigenome and
460 mutation rates in plants (Martincorena & Luscombe, 2013; Quiroz *et al.*, 2023). Further work on DNA

461 repair systems in plants is needed to clarify their role in mutation rate variation across nuclear and
462 organellar genomes.
463
464 *Evolutionary rates in land plants*
465 Across land plants, we found that nuclear genomes have evolved the most rapidly, followed by
466 chloroplast genomes and mitochondrial genomes. These results are consistent with those of
467 previous studies (Wolfe *et al.*, 1987; Drouin *et al.*, 2008; Smith, 2015). Overall, land plant nuclear
468 genomes exhibit highly dynamic evolution, with the largest genomes 2400 times the size of the
469 smallest; nuclear genomes also undergo rampant polyploidisation in land plants (Pellicer *et al.*,
470 2018). Furthermore, nuclear genomes are responsible for most cell functions, encoding between
471 25,000–40,000 genes (Heslop-Harrison & Schmidt, 2012). Thus, their high evolutionary rate, when
472 compared with the reduced rates of the chloroplast and mitochondrial genomes, is not unexpected.
473 The low evolutionary rates of nuclear and organellar genomes in gymnosperms are consistent with
474 the long generations of these taxa (Leitch & Leitch, 2012; De La Torre *et al.*, 2017). Whilst many
475 angiosperms can complete their life cycle in mere weeks, most gymnosperms take years to finish a
476 single cycle.
477
478 There was a moderate amount of among-lineage rate heterogeneity overall in nuclear and
479 chloroplast genes in the major land plant clades. Our results are consistent with previous findings of
480 high-rate heterogeneity among lineages in angiosperm mitochondrial genomes. Whilst plants have
481 drastically lower rates of mitochondrial evolution, the angiosperm mitochondrial genome is dynamic
482 and exhibits highly variable evolutionary rates (Galtier, 2011; Havird *et al.*, 2017; Petersen *et al.*,
483 2020). The inflated rates of mitochondrial evolution in lineages such as *Plantago*, *Silene*, and *Viscum*
484 have been attributed to genetic transfer from bacteria, viruses, and the nuclear and chloroplast
485 genomes (Zervas *et al.*, 2019). Indeed, the phenomenon of mitochondrial fusion is exhibited by
486 *Amborella trichopoda*, the sister taxon to all other angiosperms (Rice *et al.*, 2013). The mitochondrial
487 genome of this species has fused with the whole genomes of three green algae and a moss species,
488 and has received 82 copies of protein-coding and rRNA genes via horizontal transfer from other
489 angiosperm species (Rice *et al.*, 2013). Further insights will be gained from analysing larger amounts
490 of data, particularly additional mitochondrial data; mitochondrial genomes are publicly available for
491 only 142 species of plants, compared with 4445 chloroplast genomes (Petersen *et al.*, 2020).
492

493 *Evolutionary rates in parasitic angiosperms*

494 The parasitic flowering plants included in our study exhibited high levels of among-lineage rate
495 heterogeneity in their nuclear and organellar genomes. Rate heterogeneity was especially
496 pronounced in nuclear genes of Rafflesiaceae, in mitochondrial genes of *Loranthus*, and in
497 chloroplast genes of Orobanchaceae. Given the extreme levels of rate variation, it is perhaps
498 unsurprising that we could not detect any evolutionary rate correlations in the parasitic angiosperms
499 that we tested: *Loranthus*, Orobanchaceae, Rafflesiaceae, and *Thesium*.

500

501 Parasitism has evolved at least 12 times across the angiosperms (Westwood *et al.*, 2010; Nickrent,
502 2020), with an estimated 4750 species attacking the stems and roots of host plants for nutrition. Our
503 data sets included Rafflesiaceae, a group of the most reduced holoparasites (Molina *et al.*, 2014).
504 Holoparasites do not perform any photosynthetic function and rely on their hosts for their
505 nutritional requirements, with the most extreme form being endoparasitism. Indeed, Rafflesiaceae
506 include endoparasites such as *Sapria*, which lack an independent body and grow directly on their
507 host (Cai *et al.*, 2021). Other parasite species that we analysed occur as hemiparasites, which have
508 not lost photosynthetic function completely, and only partly rely on their host for heterotrophic
509 nutrient demands (Těšitel *et al.*, 2010). Hemiparasites can be either obligate, depending on their
510 hosts for nutrients, or facultative, where they are able to live independently of their hosts (Těšitel *et*
511 *al.*, 2010). We analysed data from obligate parasites *Loranthus*, which often reside on the stems of
512 their hosts (Liu *et al.*, 2018), and *Thesium*, which includes both obligate and facultative herbaceous
513 parasites that attach to the roots of their hosts. Orobanchaceae includes members that span the
514 range of parasitic modes, from free-living hemiparasites to holoparasites that live on their hosts and
515 leach water and nutrients directly from the hosts' roots, e.g., in desert hyacinths (Nickrent, 2020;
516 Thorogood *et al.*, 2021).

517

518 The degree of parasitism seems to be linked to the amount of chloroplast reduction. For example,
519 the holoparasitic members of Orobanchaceae have experienced widespread chloroplast gene losses,
520 with members of Rafflesiaceae being the most extreme iteration of this gene loss, as they appear to
521 have lost their chloroplast genomes entirely (Molina *et al.*, 2014; Zervas *et al.*, 2019). The
522 hemiparasitic *Viscum*, a genus of mistletoe, have lost 10–22% of their chloroplast genes compared
523 with their autotrophic relatives (Petersen *et al.*, 2015; Zervas *et al.*, 2019). These gene losses are
524 likely to be associated also with the loss of signalling and regulatory genes in the nuclear and
525 mitochondrial genomes. This may have caused the lack of evolutionary rate correlations between
526 nuclear and organellar genomes in parasitic angiosperms, given the loss of nuclear-encoded genes.

Moreover, due to the intimate nature of the host–parasite association, horizontal gene transfer is rife, especially in the mitochondrial genomes of parasite species. In family Rafflesiaceae, it was found that 24–41% of mitochondrial genes were donated from the host plant (Xi *et al.*, 2013). This provides another potential explanation for the lack of evolutionary rate correlations; the foreign genes have not undergone coordinated evolution with the native genes over millions of years.

Conclusions

We have identified correlations in evolutionary rates across the nuclear, mitochondrial, and chloroplast genomes in land plants, but not in parasitic angiosperms. These associations suggest that the evolution of the three genomes is at least partly governed by a common factor that acts upon mutation rates. Further insight into these evolutionary dynamics can be gained through detailed studies of specific genes, including nuclear and mitochondrial genes that encode products that are used in the mitochondria. Our framework can be extended to other major lineages of plants, including the green algae but also red algae. We found a weakly positive (but insignificant) correlation in a small data set of chlorophytes. If there is evidence for evolutionary rate correlations in algae, this indicates that the dynamic is ancient and consistent across all Viridiplantae. Indeed, whether rate correlations exist at an even larger scale across between the genomic compartments across the Tree of Life is unknown. This is particularly pertinent as new organelles are being discovered, such as the nitrogen-fixing organelle, the 'nitroplast' (Coale *et al.*, 2024). Another open question is whether evolutionary rate correlations would persist in other photosynthetic eukaryote lineages with plastids derived from secondary or tertiary symbioses, such as dinoflagellates (Maruyama & Kim, 2020). Uncovering the drivers of evolutionary rate correlations will allow better understanding of the causes of genomic change.

Acknowledgements

This work was supported by the Australian Research Council (DP220103265). Y.A. also acknowledges the support provided by an Australian Government Research Training Program Scholarship. The authors acknowledge the Sydney Informatics Hub and the high-performance computing facility, Artemis, at the University of Sydney for providing computing resources. We also thank Samuli Lehtonen, Glenda Cardenas Ramirez, Miguel Angel García García, Pieter Pelser, Chi Toan Le, Daniel Nickrent, Sean Graham, and Frank E Anderson for providing access to data sets.

Competing interests

There are no competing interests to report.

Author contributions

YA, HS, and SYWH designed and planned the study. YA collected, curated, and analysed the empirical data sets and performed simulations. YA wrote the manuscript, with input from HS and SYWH.

567 **References**

568 **Anderson SAS, Weir JT**. **2020**. A comparative test for divergent adaptation: inferring speciation
569 drivers from functional trait divergence. *The American Naturalist* **196**: 429–442.

570 **Asar Y, Sauquet H, Ho SYW**. **2023**. Evaluating the accuracy of methods for detecting correlated rates
571 of molecular and morphological evolution. *Systematic Biology* **72**: 1337–1356.

572 **Barreto FS, Watson ET, Lima TG, Willett CS, Edmands S, Li W, Burton RS**. **2018**. Genomic signatures
573 of mitonuclear coevolution across populations of *Tigriopus californicus*. *Nature Ecology & Evolution*
574 **2**: 1250–1257.

575 **Bechteler J, Peñaloza-Bojacá G, Bell D, Gordon Burleigh J, McDaniel SF, Christine Davis E, Sessa EB,**
576 **Bippus A, Christine Cargill D, Chantanoarrapint S, *et al.* 2023**. Comprehensive phylogenomic time
577 tree of bryophytes reveals deep relationships and uncovers gene incongruences in the last 500
578 million years of diversification. *American Journal of Botany* **110**: e16249.

579 **Belfield EJ, Brown C, Ding ZJ, Chapman L, Luo M, Hinde E, van Es SW, Johnson S, Ning Y, Zheng SJ,**
580 ***et al.* 2021**. Thermal stress accelerates *Arabidopsis thaliana* mutation rate. *Genome Research* **31**:
581 40–50.

582 **Bentolila S, Alfonso A, Hanson M**. **2002**. A pentatricopeptide repeat-containing gene restores
583 fertility to cytoplasmic male-sterile plants. *Proceedings of the National Academy of Sciences of the*
584 *United States of America* **99**: 10887–10892.

585 **Benton MJ, Wilf P, Sauquet H**. **2022**. The angiosperm terrestrial revolution and the origins of
586 modern biodiversity. *New Phytologist* **233**: 2017–2035.

587 **Bergeron LA, Besenbacher S, Zheng J, Li P, Bertelsen MF, Quintard B, Hoffman JI, Li Z, St. Leger J,**
588 **Shao C, *et al.* 2023**. Evolution of the germline mutation rate across vertebrates. *Nature* **615**: 285–
589 291.

590 **Biot-Pelletier D, Bettinazzi S, Gagnon-Arsenault I, Dubé AK, Bédard C, Nguyen THM, Fiumera HL,**
591 **Breton S, Landry CR**. **2023**. Evolutionary trajectories are contingent on mitonuclear interactions.
592 *Molecular Biology and Evolution* **40**: msad061.

593 **Boesch P, Weber-Lotfi F, Ibrahim N, Tarasenko V, Cosset A, Paulus F, Lightowlers RN, Dietrich A**.
594 **2011**. DNA repair in organelles: pathways, organization, regulation, relevance in disease and aging.
595 *Biochimica et Biophysica Acta - Molecular Cell Research* **1813**: 186–200.

596 **Bouckaert RR, Drummond AJ**. **2017**. bModelTest: Bayesian phylogenetic site model averaging and
597 model comparison. *BMC Evolutionary Biology* **17**: 42.

598 **Bouckaert R, Vaughan TG, Barido-Sottani J, Duchêne S, Fourment M, Gavryushkina A, Heled J,**
599 **Jones G, Kühnert D, De Maio N, *et al.* 2019**. BEAST 2.5: an advanced software platform for Bayesian
600 evolutionary analysis. *PLOS Computational Biology* **15**: e1006650.

601 **Bromham L, Hua X, Lanfear R, Cowman PF**. **2015**. Exploring the relationships between mutation
602 rates, life history, genome size, environment, and species richness in flowering plants. *The American*
603 *Naturalist* **185**: 507–524.

604 **Bromham L, Woolfit M, Lee MSY, Rambaut A**. **2002**. Testing the relationship between
605 morphological and molecular rates of change along phylogenies. *Evolution* **56**: 1921–1930.

606 **Bui MQ, Schmidt HA, Chernomor O, Schrempf D, Woodhams MD, von Haeseler A, Lanfear R**. **2020**.
607 IQ-TREE 2: new models and efficient methods for phylogenetic inference in the genomic era.
608 *Molecular Biology and Evolution* **37**: 1530–1534.

609 **Burton RS, Pereira RJ, Barreto FS**. **2013**. Cytonuclear genomic interactions and hybrid breakdown.
610 *Annual Review of Ecology, Evolution, and Systematics* **44**: 281–302.

611 **Cai L, Arnold BJ, Xi Z, Khost DE, Patel N, Hartmann CB, Manickam S, Sasirat S, Nikolov LA, Mathews**
612 **S, *et al.* 2021**. Deeply altered genome architecture in the endoparasitic flowering plant Sapria
613 himalayana Griff. (Rafflesiaceae). *Current Biology* **31**: 1002-1011.e9.

614 **Cantino PD, Doyle JA, Graham SW, Judd WS, Olmstead RG, Soltis DE, Soltis PS, Donoghue MJ**.
615 **2007**. Towards a phylogenetic nomenclature of Tracheophyta. *Taxon* **56**: E1–E44.

616 **Chen Z, Zhao N, Li S, Grover CE, Nie H, Wendel JF, Hua J**. **2017**. Plant mitochondrial genome
617 evolution and cytoplasmic male sterility. *Critical Reviews in Plant Sciences* **36**: 55–69.

618 **Coale TH, Loconte V, Turk-Kubo KA, Vanslembrouck B, Mak WKE, Cheung S, Ekman A, Chen J-H,**
619 **Hagino K, Takano Y, *et al.* 2024**. Nitrogen-fixing organelle in a marine alga. *Science* **384**: 217–222.

620 **David P, Degletagne C, Saclier N, Jennan A, Jarne P, Plénet S, Konecny L, François C, Guéguen L,**
621 **Garcia N, *et al.* 2022**. Extreme mitochondrial DNA divergence underlies genetic conflict over sex
622 determination. *Current Biology* **32**: 2325-2333.e6.

623 **Davies TJ, Savolainen V, Chase MW, Moat J, Barracloug TG**. **2004**. Environmental energy and
624 evolutionary rates in flowering plants. *Proceedings of the Royal Society B: Biological Sciences* **271**:
625 2195–2200.

626 **Delph LF, Touzet P, Bailey MF**. **2007**. Merging theory and mechanism in studies of gynodioecy.
627 *Trends in Ecology & Evolution* **22**: 17–24.

628 **Drouin G, Daoud H, Xia J**. **2008**. Relative rates of synonymous substitutions in the mitochondrial,
629 chloroplast and nuclear genomes of seed plants. *Molecular Phylogenetics and Evolution* **49**: 827–
630 831.

631 **Drummond AJ, Ho SYW, Phillips MJ, Rambaut A**. **2006**. Relaxed phylogenetics and dating with
632 confidence. *PLOS Biology* **4**: e88.

633 **Duchêne D, Bromham L**. **2013**. Rates of molecular evolution and diversification in plants: chloroplast
634 substitution rates correlate with species-richness in the Proteaceae. *BMC Evolutionary Biology* **13**:
635 65.

636 **Enquist BJ, Feng X, Boyle B, Maitner B, Newman EA, Jørgensen PM, Roehrdanz PR, Thiers BM,**
637 **Burger JR, Corlett RT, *et al.* 2019**. The commonness of rarity: global and future distribution of rarity
638 across land plants. *Science Advances* **5**: eaaz0414.

639 **Felsenstein J**. **1985**. Phylogenies and the comparative method. *The American Naturalist* **125**: 1–15.

640 **Fernández P, Amice R, Bruy D, Christenhusz MJM, Leitch IJ, Leitch AL, Pokorny L, Hidalgo O, Pellicer**
641 **J**. **2024**. A 160 Gbp fork fern genome shatters size record for eukaryotes. *iScience* **27**: 109889.

642 **Formaggioni A, Plazzi F, Passamonti M**. **2022**. Mito-nuclear coevolution and phylogenetic artifacts:
643 the case of bivalve mollusks. *Scientific Reports* **12**: 11040.

644 **Forsythe ES, Williams AM, Sloan DB**. **2021**. Genome-wide signatures of plastid-nuclear coevolution
645 point to repeated perturbations of plastid proteostasis systems across angiosperms. *Plant Cell* **33**:
646 980–997.

647 **Freckleton RP**. **2000**. Phylogenetic tests of ecological and evolutionary hypotheses: checking for
648 phylogenetic independence. *Functional Ecology* **14**: 129–134.

649 **Fujii S, Bond CS, Small ID**. **2011**. Selection patterns on restorer-like genes reveal a conflict between
650 nuclear and mitochondrial genomes throughout angiosperm evolution. *Proceedings of the National*
651 *Academy of Sciences, USA* **108**: 1723–1728.

652 **Galtier N**. **2011**. The intriguing evolutionary dynamics of plant mitochondrial DNA. *BMC Biology* **9**: 9–
653 11.

654 **Garland T, Harvey PH, Ives AR**. **1992**. Procedures for the analysis of comparative data using
655 phylogenetically independent contrasts. *Systematic Biology* **41**: 18–32.

656 **Garren ST**. **2017**. Permutation tests for nonparametric statistics using R. *Asian Research Journal of*
657 *Mathematics* **5**: 1–8.

658 **Graham SW, Lam VKY, Merckx VSFT**. **2017**. Plastomes on the edge: the evolutionary breakdown of
659 mycoheterotroph plastid genomes. *New Phytologist* **214**: 48–55.

660 **Greiner S, Sobanski J, Bock R**. **2015**. Why are most organelle genomes transmitted maternally?
661 *BioEssays* **37**: 80–94.

662 **Havird JC, Noe GR, Link L, Torres A, Logan DC, Sloan DB, Chicco AJ**. **2019**. Do angiosperms with
663 highly divergent mitochondrial genomes have altered mitochondrial function? *Mitochondrion* **49**: 1–
664 11.

665 **Havird JC, Trapp P, Miller CM, Bazos I, Sloan DB**. **2017**. Causes and consequences of rapidly evolving
666 mtDNA in a plant lineage. *Genome Biology and Evolution* **9**: 323–336.

667 **Heslop-Harrison JS (Pat), Schmidt T**. **2012**. Plant nuclear genome composition. In: eLS.
668 https://doi.org/10.1002/9780470015902.a0002014.pub.

669 **Higgins JJ**. **2004**. *Introduction to Modern Nonparametric Statistics.* Pacific Grove, CA: Brooks/Cole.

670 **Hill GE**. **2016**. Mitonuclear coevolution as the genesis of speciation and the mitochondrial DNA
671 barcode gap. *Ecology and Evolution* **6**: 5831–5842.

672 **Hill GE**. **2020**. Mitonuclear compensatory coevolution. *Trends in Genetics* **36**: 403–414.

673 **Kaur P, Kaila T, Dhkal M, Gaikwad K**. **2022**. Chapter 26 – Chloroplast genome and plant–virus
674 interaction. In: Sharma P, Yadav D, Gaur RK, eds. Bioinformatics in Agriculture. Academic Press, 419–
675 436.

676 **Khachaturyan M, Santer M, Reusch TBH, Dagan T**. **2024**. Heteroplasmy is rare in plant mitochondria
677 compared to plastids despite similar mutation rates. *Molecular Biology andE* **41**: msae135.

678 **De La Torre AR, Li Z, Van De Peer Y, Ingvarsson PK**. **2017**. Contrasting rates of molecular evolution
679 and patterns of selection among gymnosperms and flowering plants. *Molecular Biology and*
680 *Evolution* **34**: 1363–1377.

681 **Lancaster LT**. **2010**. Molecular evolutionary rates predict both extinction and speciation in
682 temperate angiosperm lineages. *BMC Evolutionary Biology* **10**: 162.

683 **Lanfear R, Ho SYW, Jonathan Davies T, Moles AT, Aarssen L, Swenson NG, Warman L, Zanne AE,**
684 **Allen AP**. **2013**. Taller plants have lower rates of molecular evolution. *Nature Communications* **4**:
685 1879.

686 **Lanfear R, Ho SYW, Love D, Bromham L**. **2010**. Mutation rate is linked to diversification in birds.
687 *Proceedings of the National Academy of Sciences, USA* **107**: 20423–20428.

688 **Leitch AR, Leitch IJ**. **2012**. Ecological and genetic factors linked to contrasting genome dynamics in
689 seed plants. *New Phytologist* **194**: 629–646.

690 **Li W-H, Ellsworth DL, Krushkal J, Chang BH-J, Hewett-Emmett D**. **1996**. Rates of nucleotide
691 substitution in primates and rodents and the generation–time effect hypothesis. *Molecular*
692 *Phylogenetics and Evolution* **5**: 182–187.

693 **Lian Q, Li S, Kan S, Liao X, Huang S, Sloan DB, Wu Z**. **2024**. Association analysis provides insights into
694 plant mitonuclear interactions. *Molecular Biology and Evolution* **41**: msae028.

695 **Liu B, Le CT, Barrett RL, Nickrent DL, Chen Z, Lu L, Vidal-Russell R**. **2018**. Historical biogeography of
696 Loranthaceae (Santalales): diversification agrees with emergence of tropical forests and radiation of
697 songbirds. *Molecular Phylogenetics and Evolution* **124**: 199–212.

698 **Lu Z, Cui J, Wang L, Teng N, Zhang S, Lam HM, Zhu Y, Xiao S, Ke W, Lin J, *et al.* 2021**. Genome-wide
699 DNA mutations in Arabidopsis plants after multigenerational exposure to high temperatures.
700 *Genome Biology* **22**: 160.

701 **Martin W**. **2003**. Gene transfer from organelles to the nucleus: Frequent and in big chunks.
702 *Proceedings of the National Academy of Sciences, USA* **100**: 8612–8614.

703 **Martin W, Herrmann RG**. **1998**. Gene transfer from organelles to the nucleus: how much, what
704 happens, and why? *Plant Physiology* **118**: 9–17.

705 **Martincorena I, Luscombe NM**. **2013**. Non-random mutation: the evolution of targeted
706 hypermutation and hypomutation. *BioEssays* **35**: 123–130.

707 **Maruyama S, Kim E**. **2020**. Evolution of photosynthetic eukaryotes; Current opinion, perplexity, and
708 a new perspective. In: Kloc M, ed. Symbiosis: Cellular, Molecular, Medical and Evolutionary Aspects.
709 Springer, 337–351.

710 **Molina J, Hazzouri KM, Nickrent D, Geisler M, Meyer RS, Pentony MM, Flowers JM, Pelser P,**
711 **Barcelona J, Inovejas SA, *et al.* 2014**. Possible loss of the chloroplast genome in the parasitic
712 flowering plant *Rafflesia lagascae* (Rafflesiaceae). *Molecular Biology and Evolution* **31**: 793–803.

713 **Morley SA, Nielsen BL**. **2017**. Plant mitochondrial DNA. *Frontiers in Bioscience - Landmark* **22**: 1023–
714 1132.

715 **Morris JL, Puttick MN, Clark JW, Edwards D, Kenrick P, Pressel S, Wellman CH, Yang Z, Schneider H,**
716 **Donoghue PCJ**. **2018**. The timescale of early land plant evolution. *Proceedings of the National*
717 *Academy of Sciences, USA* **115**: E2274–E2283.

718 **Nickrent DL**. **2020**. Parasitic angiosperms: how often and how many? *Taxon* **69**: 5–27.

719 **Nie Y, Foster CSP, Zhu T, Yao R, Duchene DA, Ho SYW, Zhong B**. **2020**. Accounting for uncertainty in
720 the evolutionary timescale of green plants through clock-partitioning and fossil calibration
721 strategies. *Systematic Biology* **69**: 1–16.

722 **One Thousand Plant Transcriptomes I**. **2019**. One thousand plant transcriptomes and the
723 phylogenomics of green plants. *Nature* **574**: 679–685.

724 **Pellicer J, Hidalgo O, Dodsworth S, Leitch IJ**. **2018**. Genome size diversity and its impact on the
725 evolution of land plants. *Genes (Basel)* **9**: 88.

726 **Petersen G, Anderson B, Braun H-P, Meyer EH, Møller IM**. **2020**. Mitochondria in parasitic plants.
727 *Mitochondrion* **52**: 173–182.

728 **Petersen G, Cuenca A, Seberg O**. **2015**. Plastome Evolution in Hemiparasitic Mistletoes. *Genome*
729 *Biology and Evolution* **7**: 2520–2532.

730 **Petit RJ, Hampe A**. **2006**. Some evolutionary consequences of being a tree. *Annual Review of*
731 *Ecology, Evolution, and Systematics* **37**: 187–214.

732 **Piccinini G, Iannello M, Puccio G, Plazzi F, Havird JC, Ghiselli F**. **2021**. Mitonuclear coevolution, but
733 not nuclear compensation, drives evolution of OXPHOS complexes in bivalves. *Molecular Biology and*
734 *Evolution* **38**: 2597–2614.

735 **Quiroz D, Lensink M, Kliebenstein DJ, Grey Monroe J**. **2023**. Causes of mutation rate variability in
736 plant genomes. *Annual Review of Plant Biology* **74**: 751–775.

737 **Rambaut A, Drummond AJ, Xie D, Baele G, Suchard MA**. **2018**. Posterior Summarization in Bayesian
738 Phylogenetics Using Tracer 1.7. *Systematic Biology* **67**: 901–904.

739 **Ramírez-Barahona S, Sauquet H, Magallón S**. **2020**. The delayed and geographically heterogeneous
740 diversification of flowering plant families. *Nature Ecology & Evolution* **4**: 1232–1238.

741 **Rice DW, Alverson AJ, Richardson AO, Young GJ, Sanchez-Puerta MV, Munzinger J, Barry K, Boore**
742 **JL, Zhang Y, DePamphilis CW, *et al.* 2013**. Horizontal transfer of entire genomes via mitochondrial
743 fusion in the angiosperm *Amborella*. *Science* **342**: 1468–1473.

744 **Rockenbach K, Havird JC, Grey Monroe J, Triant DA, Taylor DR, Sloan DB**. **2016**. Positive selection in
745 rapidly evolving plastid-nuclear enzyme complexes. *Genetics* **204**: 1507–1522.

746 **Ruhfel BR, Gitzendanner MA, Soltis PS, Soltis DE, Burleigh JG**. **2014**. From algae to angiosperms–
747 inferring the phylogeny of green plants (Viridiplantae) from 360 plastid genomes. *BMC Evolutionary*
748 *Biology* **14**: 23.

749 **Sanchez-Puerta MV, Ceriotti LF, Gatica-Soria LM, Roulet ME, Garcia LE, Sato HA**. **2023**. Beyond
750 parasitic convergence: unravelling the evolution of the organellar genomes in holoparasites. *Annals*
751 *of Botany* **132**: 909–928.

752 **Sauquet H, Ramírez-Barahona S, Magallón S**. **2022**. What is the age of flowering plants? (R Melzer,
753 Ed.). *Journal of Experimental Botany* **73**: 3840–3853.

754 **Sloan DB, Havird JC, Sharbrough J**. **2017**. The on-again, off-again relationship between
755 mitochondrial genomes and species boundaries. *Molecular Ecology* **26**: 2212–2236.

756 **Sloan DB, Triant DA, Wu M, Taylor DR**. **2014**. Cytonuclear interactions and relaxed selection
757 accelerate sequence evolution in organelle ribosomes. *Molecular Biology and Evolution* **31**: 673–682.

758 **Smith DR**. **2015**. Mutation rates in plastid genomes: they are lower than you might think. *Genome*
759 *Biology and Evolution* **7**: 1227–1234.

Soltis PS, Folk RA, Soltis DE. **2019**. Darwin review: angiosperm phylogeny and evolutionary radiations. *Proceedings of the Royal Society B: Biological Sciences* **286**: 20190099.

Tao M, Chen J, Cui C, Xu Y, Xu J, Shi Z, Yun J, Zhang J, Ou G-Z, Liu C, *et al.* 2024. Identification of a longevity gene through evolutionary rate covariation of insect mito-nuclear genomes. *Nature Aging*: https://doi.org/10.1038/s43587-024-00641-z.

Těšitel J, Plavcová L, Cameron DD. **2010**. Interactions between hemiparasitic plants and their hosts. *Plant Signaling & Behavior* **5**: 1072–1076.

Thorogood CJ, Leon CJ, Lei D, Aldughayman M, Huang L, Hawkins JA. **2021**. Desert hyacinths: An obscure solution to a global problem? *PLANTS, PEOPLE, PLANET* **3**: 302–307.

Tyszka AS, Bretz EC, Robertson HM, Woodcock-Girard MD, Ramanauskas K, Larson DA, Stull GW, Walker JF. **2023**. Characterizing conflict and congruence of molecular evolution across organellar genome sequences for phylogenetics in land plants. *Frontiers in Plant Science* **14**: 1125107.

Wang L-G, Lam TT-Y, Xu S, Dai Z, Zhou L, Feng T, Guo P, Dunn CW, Jones BR, Bradley T, *et al.* 2020. Treeio: an R package for phylogenetic tree input and output with richly annotated and associated data. *Molecular Biology and Evolution* **37**: 599–603.

Wang S, Ore MJ, Mikkelsen EK, Lee-Yaw J, Toews DPL, Rohwer S, Irwin D. **2021**. Signatures of mitonuclear coevolution in a warbler species complex. *Nature Communications* **12**: 4279.

Wang J, Xu G, Ning Y, Wang X, Wang GL. **2022**. Mitochondrial functions in plant immunity. *Trends in Plant Science* **27**: 1063–1076.

Watanabe K, Yamada N, Takeuchi Y. **2006**. Oxidative DNA damage in cucumber cotyledons irradiated with ultraviolet light. *Journal of Plant Research* **119**: 239–246.

Weaver RJ, Rabinowitz S, Thueson K, Havird JC. **2022**. Genomic signatures of mitonuclear coevolution in mammals. *Molecular Biology and Evolution* **39**: msac233.

Welch JJ, Waxman D. **2008**. Calculating independent contrasts for the comparative study of substitution rates. *Journal of Theoretical Biology* **251**: 667–678.

Westwood JH, Yoder JI, Timko MP, dePamphilis CW. **2010**. The evolution of parasitism in plants. *Trends in Plant Science* **15**: 227–235.

Williams AM, Friso G, van Wijk KJ, Sloan DB. **2019**. Extreme variation in rates of evolution in the plastid Clp protease complex. *Plant Journal* **98**: 243–259.

Wolfe KH, Li WH, Sharp PM. **1987**. Rates of nucleotide substitution vary greatly among plant mitochondrial, chloroplast, and nuclear DNAs. *Proceedings of the National Academy of Sciences, USA* **84**: 9054–9058.

Xi Z, Wang Y, Bradley RK, Sugumaran M, Marx CJ, Rest JS, Davis CC. **2013**. Massive mitochondrial gene transfer in a parasitic flowering plant clade. *PLOS Genetics* **9**: e1003265.

Yan Z, Ye G, Werren JH. **2019**. Evolutionary rate correlation between mitochondrial-encoded and mitochondria-associated nuclear-encoded proteins in insects. *Molecular Biology and Evolution* **36**: 1022–1036.

Yang Y, Forsythe ES, Ding YM, Zhang DY, Bai WN. **2023**. Genomic analysis of plastid-nuclear interactions and differential evolution rates in coevolved genes across Juglandaceae species. *Genome Biology and Evolution* **15**: evad145.

800 **Zeng L, Zhang Q, Sun R, Kong H, Zhang N, Ma H**. **2014**. Resolution of deep angiosperm phylogeny
801 using conserved nuclear genes and estimates of early divergence times. *Nature Communications* **5**:
802 4956.

803 **Zervas A, Petersen G, Seberg O**. **2019**. Mitochondrial genome evolution in parasitic plants. *BMC*
804 *Evolutionary Biology* **19**: 87.

805 **Zhang J, Ruhlman TA, Sabir J, Blazier JC, Jansen RK**. **2015**. Coordinated rates of evolution between
806 interacting plastid and nuclear genes in geraniaceae. *Plant Cell* **27**: 563–573.

807 **Zwonitzer KD, Tressel LG, Wu Z, Kan S, Broz AK, Mower JP, Ruhlman TA, Jansen RK, Sloan DB,**
808 **Havird JC**. **2024**. Genome copy number predicts extreme evolutionary rate variation in plant
809 mitochondrial DNA. *Proceedings of the National Academy of Sciences, USA* **121**: e2317240121.

810